INFLUENCE OF THE FLAME FRONT ON THE FLOW INSIDE A COMBUSTION CHAMBER

Bogdan GHERMAN[1], Virgil STANCIU[2]

In această lucrare este studiată influența frontului de flacara asupra curgerii într-o camera de ardere de aviatie experimentală. Studiul a fost realizat folosind simularea numerică bazată pe integrarea numerică a ecuațiilor Navier-Stokes cu modelul de turbulenta k-ε si modelul de ardere Eddy Dissipation. Analiza realizată a avut doua părți: una in care s-a studiat curgerea în interiorul camerei, fără ardere si a doua cu ardere. Comparatia între cele doua analize arata o modificare a zonei de recirculare, ce se formează în centrul camerei, în sensul că grosimea acesteia se reduce cu approx 15 % şi se alungeste cu 10 % pe direcția axială, în cazul cu ardere.

In this paper it is studied the influence of the flame front on the flow inside of a combustion chamber. The study has been carried out using a steady state numerical simulation based on Navier-stokes equation with k-ε turbulence model and Eddy dissipation combustion model. The analysis was done in two stages: in the first one it was studied the flow inside the combustion chamber without combustion and the second stage with combustion. Comparisons between the two stages showed a modification of the recirculation zone (that forms at the center of the chamber) by approx. 15% in thickness and almost 10% in length in axial direction in the case with combustion.

Key words: flame front, recirculation zone, CFD, combustion chamber

Nomenclature

$_I$	kinematic diffusivity [m^2/s]
h	specific thermodynamic enthalpy [J/kg]
k	specific turbulent kinetic energy per unit mass [m^2/s^2]
w	molecular weight [$kg/kmol$]
p	pressure [N/m^2]
R	universal gas constant [J/kgK]
S_I	is the source term due to chemical reaction rate involving component I
T	temperature [K]; u velocity [m]

[1] Eng., Romanian Research and Development Institute for Gas Turbines, COMOTI, Romania, e-mail: bogdan.gherman@comoti.ro
[2] Prof., Faculty of Aerospace Engineering, University POLITEHNICA of Bucharest, Romania, e-mail: v_stanciu@aero.pub.ro, vvirgilstanciu@yahoo.com

P_k turbulence production due to viscous forces; t time [s]
R_K elementary reaction rate of progress for reaction k
W_I molar mass [$kg/kmol$]; Y mass fraction [-]
C_{S1} model constant [-] ; C_{S2} model constant [-]

Greek characters

δ Kronecker delta [-]
ε dissipation rate of the turbulent kinetic energy per unit mass [m^2/s^3]
μ dynamic viscosity [$kg/(ms)$]; ν kinematic viscosity [m^2/s]
ρ density [kg/m^3]; ν_{kI} stoichiometric coefficient for component I
τ_{ij} turbulent stress tensor [m^2/s^2]; σ_k model constant [-]
σ_ε model constant [-]; Γ_i diffusion coefficient of component I [m^2/s]

Dimensionless numbers

Pr Prandtl number

Statistical quantities

$\overline{\phi}$ time or ensemble average of variable ϕ
ϕ' fluctuating part of variable ϕ; $\widetilde{\phi}$ filtered variable ϕ

1. Introduction

In a combustor, the main concerns are the fuel-air mixing and the flame stability. A better control of these two phenomena can improve the combustion efficiency and decrease pollutant emissions. In practical combustion devices, there are two common ways to stabilize the flame front: through the use of bluff bodies or swirling flows. In the case of a bluff body, the recirculation zone occurs behind it, and the flame front is formed downstream of the aft edges of the bluff body. This solution is rather complicated and implies complex geometries and high temperature resistant materials for the bluff body. Also, some constructive solutions require even bluff body cooling. The stability of the flame front is assured by the recirculation zone behind the bluff body, and the flame position is determined by the bluff body geometry and position, as well as upstream flow velocity [6]. However, the degree of fuel and air mixing upstream of the bluff body is rather small. Another way to stabilize the flame front is through swirling flows which can be separated in two categories: a) swirling flows without vortex breakdown and b) swirling flows with vortex breakdown [8]. In the first category the flame front stabilization occurs only with linear decrease of the mean velocity, downstream of the burner throat [9] and the flame is situated in the place where local turbulent flame speed matches local flow velocity. An advantage of this

method is that there is no shear turbulence. In the case of the swirling flow with vortex breakdown, the flame stability is assured by a recirculation zone which is formed due to a combination of fuel and air flow angles and their different velocities at the combustor inlet [2]. When a strong swirl is created at the inlet of the combustor, it can be observed that the vortex structure remains almost unchanged in the axial direction for some distance downstream, followed by an abrupt change in the vortical structure, accompanied by a retardation of the flow in the axial direction and a corresponding divergence of the streamlines close to the device axis [1]. The phenomenon is known in the literature as the vortex breakdown [7] it is known to create a recirculation zone in the jet axis region [2].

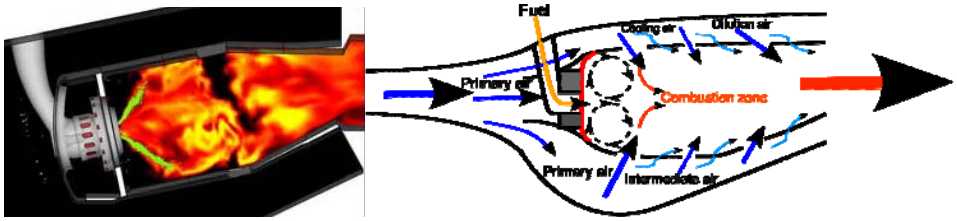

Fig. 1 Types of combustion chamber
(wikipedia & www.stanford.edugroupcitssimulationpw_combustors)

This recirculation zone is formed in the primary zone of the combustor (Fig. 1) helping at anchoring the flame and enhancing the turbulent mixing between the air and fuel.

This recirculation zone is formed in the primary zone of the combustor and its position is determined by the magnitude and direction of the fuel and air inlet velocities. The co-annular swirl configuration of the fuel and air inlets produces shear layers that are inherently unstable and increases the fuel and air mixing prior to combustion. In some situations, even counter rotating jets may be considered, in order to further enhance the fuel and air mixing. Depending on the swirl angle, the flame front in a combustor can be either tear shaped or cone shaped and the accurate prediction of a swirling flow will improve the combustion systems design. [3]

In this paper, the study is focused on the behavior of the recirculation zone formed due to a swirling flow with a vortex break down in a combustion chamber, and the effect of combustion process on the flow inside the combustion chamber particularly on the recirculation zones.

2. Mathematical Model

This study was carried out using a commercial CFD code, Ansys CFX, using a steady state approach because this study was design in two stages, a

steady state analysis and an unsteady analysis using LES method. In this paper is presented only the steady state approach.

For this study, the flow is assumed compressible, the equations that govern the flow are written in Reynolds averaged form, time and mass averaged [4], being, in the repeated indices summation convention:

The Continuity Equation**:**

$$\frac{\partial \overline{\rho}}{\partial t} + \frac{\partial \overline{\rho}\widetilde{u}_j}{\partial x_j} = 0 \tag{1}$$

The Momentum Equations:

$$\frac{\partial \overline{\rho}\widetilde{u}_i}{\partial t} + \frac{\partial \overline{\rho}(\widetilde{u}_i\widetilde{u}_j)}{\partial x_j} = -\frac{\partial \overline{p}}{\partial x_i} + \frac{\partial}{\partial x_j}\left(\overline{\tau_{ij}} - \overline{\rho u_i' u_j'}\right) \tag{2}$$

, where

$$\overline{\tau_{ij}} = \mu\left[\frac{\partial \widetilde{u}_i}{\partial x_j} + \frac{\partial \widetilde{u}_j}{\partial x_i} - \frac{2}{3}\delta_{ij}\left(\frac{\partial \widetilde{u}_k}{\partial x_k}\right)\right],$$

represents the stress tensor.

The Total Energy Equation:

$$\frac{\partial}{\partial t}\left(\overline{\rho}\widetilde{h}\right) + \frac{\partial\left(\overline{\rho}\widetilde{u}_j\widetilde{h}\right)}{\partial x_j} = \frac{\partial \overline{p}}{\partial t} + \frac{\partial}{\partial x_j}\left(\overline{\frac{\mu}{\Pr}\frac{\partial h}{\partial x_j}}\right) + \overline{\tau}_{ij}\frac{\partial \widetilde{u}_j}{\partial x_j} + \frac{\partial}{\partial x_j}\left(-\overline{\rho h' u_j'}\right), \tag{3}$$

where h is the enthalpy.

$h = \sum h_m Y$, $\quad h_I = \Delta h_f^0 + \int_{T_0}^{T} C_p(T)dT$, $I = 1, N$, N = number of species

Scalar transport Equation:

This equation is a general advection-diffusion equation and it is necessary to solve it in terms of mass fraction to establish the fluid mixture. And it is used for the transport of five species, namely CH_4, O_2, CO_2, H_2O and NO.

$$\frac{\partial\left(\overline{\rho}\widetilde{Y}_I\right)}{\partial t} + \frac{\partial\left(\overline{\rho}\widetilde{u}_j\widetilde{Y}_I\right)}{\partial x_j} = \frac{\partial}{\partial x_j}\left(\Gamma_{I_{eff}}\frac{\partial Y_I}{\partial x_j}\right) + S_I\,, \tag{4}$$

$\widetilde{Y}_I = \dfrac{\widetilde{\overline{\rho}}_i}{\rho}$,

S_I – is the source term due to chemical reaction rate involving component I,

$S_I = W_I \sum_{k=1}^{K}(\nu_{kI}'' - \nu_{kI}')R_K$,

ν_{kI} - is the stoichiometric coefficient for component *I* in the elementary reaction *k*

R_K – is the elementary reaction rate of progress for reaction k, and is calculated using Eddy Dissipation model

$$\Gamma_{I_{eff}} = \Gamma_I + \frac{\mu_t}{Sc_t}, \tag{5}$$

$\Gamma_I = \rho D_I$, D_I – kinematic diffusivity

Ideal Gas Equation of State:

$$\widetilde{\rho} = \frac{w\left(\widetilde{p} + p_{ref}\right)}{R_0 \widetilde{T}}, \tag{6}$$

where w is the molecular weight

Turbulence model used in this case is known for its robustness, cost effectiveness and reasonable accuracy but also for its challenges regarding adverse pressure gradients and boundary layer separation [14], [15]. But, nevertheless, the various forms of the k-ε model have been in use for several decades with reasonable results, and it has become the most widely used model for industrial applications. Many recent studies are trying to use and further develop the RANS models [10], [11], [12], [13], [14].

The k-ε two-equation turbulence model is employed to close the correlation type terms that appears in the above equations. The model uses the gradient diffusion hypothesis to relate the Reynolds stresses to the mean velocity gradients and the turbulent viscosity. The turbulent viscosity is modeled as the product of turbulent velocity and turbulent length scale.

In the two-equation class models, the turbulence velocity scale is computed from the turbulent kinetic energy, which is provided by numerically solving its transport equation along with the governing equations presented earlier. The turbulent length scale is estimated from two properties of the turbulence field, in this case the turbulent kinetic energy, k, and its dissipation rate, ε. The dissipation rate of the turbulent kinetic energy is also provided by numerically solving its transport equation.

$$\frac{\partial(\rho k)}{\partial t} + \nabla(\rho U k) = \nabla\left[\left(\mu + \frac{\mu_t}{\sigma_k}\right)\nabla k\right] + P_k - \rho\varepsilon \tag{7}$$

$$\frac{\partial(\rho \varepsilon)}{\partial t} + \nabla(\rho U \varepsilon) = \nabla\left[\left(\mu + \frac{\mu_t}{\sigma_\varepsilon}\right)\nabla \varepsilon\right] + \frac{\varepsilon}{k}\left(C_{S_1} P_k - C_{S_2}\rho\varepsilon\right) \tag{8}$$

where C_{S1}, C_{S2} , σ_k, σ_ε are model constants, and P_k is the turbulence production due to viscous forces which is modeled using the following formula [3]:

$$P_k = \mu_t \nabla U\left(\nabla U + \nabla U^T\right) - \frac{2}{3}\nabla U\left(3\mu_t \nabla U + \rho k\right) \tag{9}$$

These equations are discretized using a second order upwind scheme.

For combustion modeling Eddy Dissipation model was employed [4]. For this model it is sufficient to have fuel and oxidant available in the control volume for combustion to occur. The eddy dissipation model is based on the concept that chemical reaction is fast relative to the transport processes in the flow. When reactants mix at the molecular level, they instantaneously form products. The model assumes that the reaction rate may be related directly to the time required to mix reactants at the molecular level.

The convergence is satisfied when the following criteria are met:
- the residuals for pressure are under 10^{-5};
- the inlet mass flow has the same value as the one from the outlet;
- the residuals do not decrease or increase anymore, they remain at the same level.

3. Problem setup and boundary conditions of the numerical simulations

The experimental chamber simulated having 251 mm in length and approximately 120 mm wide has been simulated numerically in two distinct situations:

First a non - reactive case, where the computational domain has been discretized using a computational grid of around 4.5 million cells and 800.000 nodes, with a resolution of 1 mm close to the combustor injector.

And second, a case where combustion has been discretized using a computational grid of 5.5 million cells and 1.000.000 nodes, with two local refinements (Fig. 1b) with a resolution of 0.25 mm around the injector, 0.4 mm in the first part of the combustion chamber.

For both cases, an unstructured grid had been used (Fig. 2) because the complexity of the combustion chamber makes the problem time expensive for a structured grid. Also, in order to be able to control the grid resolution in the areas of interest, local refinements have been used in the hot case [4]. The local refinements are used in the area with high velocities and in the area of the primary recirculation zone. Also the cell size is corroborated with the geometry size.

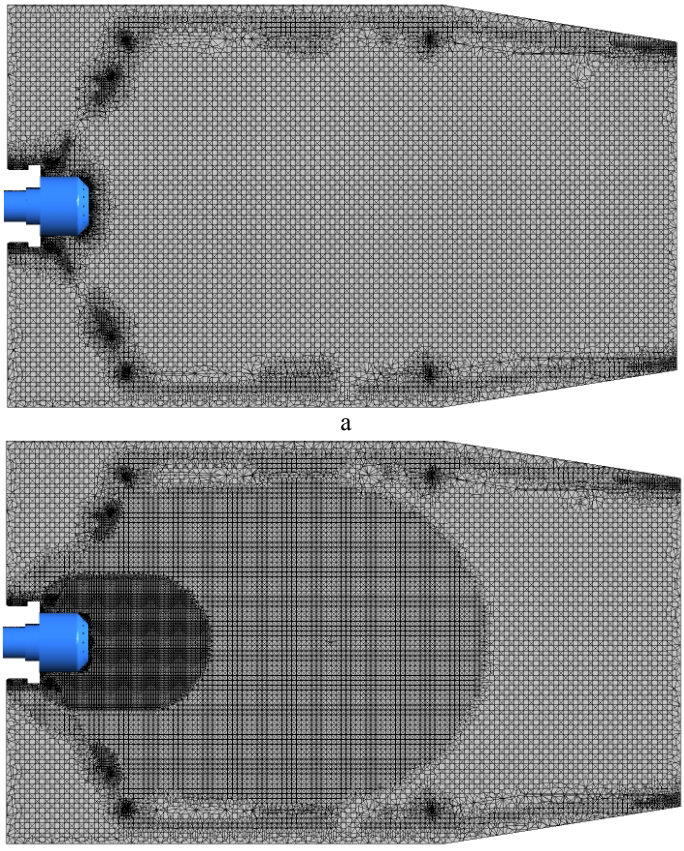

a

b

Fig. 2 Cells distribution in the discretization domain: (a) cold case, (b) hot case

The reference pressure is the atmospheric pressure, 101325 Pa.
The boundary conditions imposed at the two inlets are (Fig. 2):
The fuel inlet (both for the reactive and for the non - reactive case):
Fuel type: methane.
Fuel mass flow rate: 0.0015 kg/s – where ρU is kept constant
Fuel temperature: 288 K
The velocity is computed at inlet as a function of mass flow, temperature and reference pressure.
The air inlet:
Air mass flow rate: 4.3 kg/s – where ρU is kept constant
Air temperature: 288 K
The velocity is computed at inlet as a function of mass flow, temperature and reference pressure.
At the exit, static pressure is 10.5 bara on the main outflow, and 11 bara on the secondary outflow (Fig. 3).

The solid walls were considered adiabatic (no heat transfer), impermeable and with no-slip-(zero velocity at the wall).

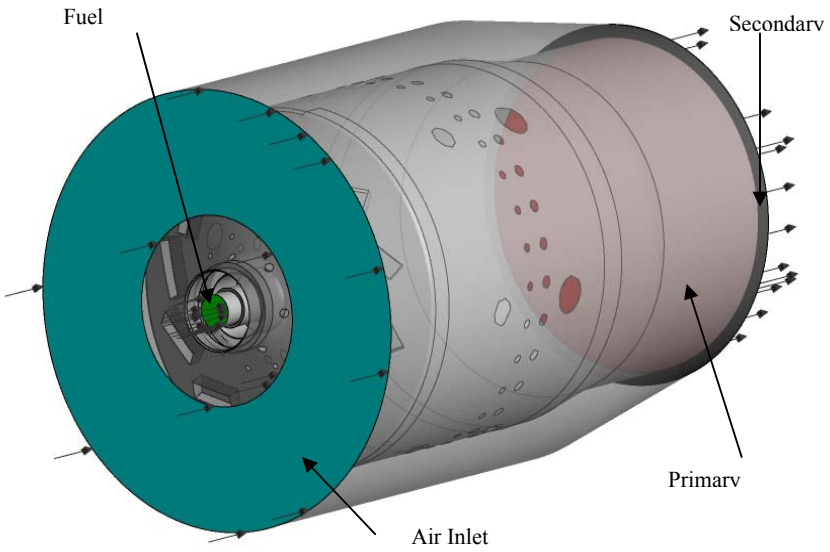

Fig. 3 Boundary condition definition on the combustor

4. Results and Discussion

The results show major differences between the two simulated cases.

The recirculation zone that forms due to the swirl inside the combustion chamber suffers obvious modifications between the two cases. In Figure 4 it can be observed that the main recirculation zone forms in the middle of the combustor and it is situated in the primary zone of the combustor. Also, the stagnation point of the recirculation zone is situated on the combustor axis, at a distance of approximately 70 mm downstream of the swirler in the non-reactive case and at approximately 80 mm in the reactive case. The swirl number also changes from 0.387 in the cold case to 0.108 in the hot case, measured at 20 mm from the injector.

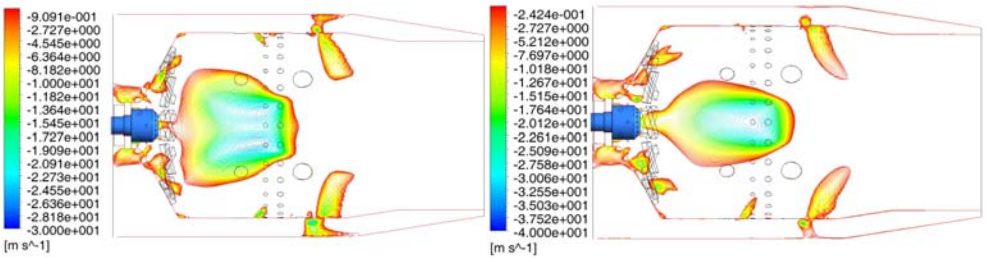

a b

Fig. 4 Isocontour of the negative axial velocity in the domain, (a) cold case and (b) hot case

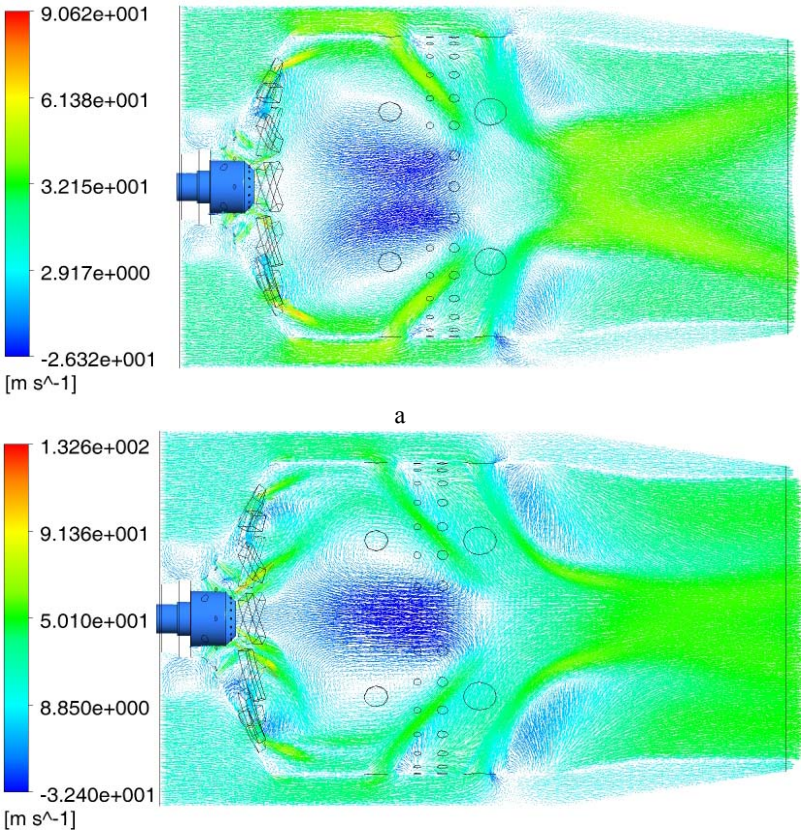

a

b

Fig. 5 Vector field (detailed view), (a) cold case and (b) hot case

The vectors, shown in Fig. 5, highlight the recirculation zones in the domain and their vertex core. A first obvious difference between the reactive and the non reactive case is the possibility to see, in the hot case, the jet that forms at the injector. As for the vertex core position it is possible to see that the position of it changes in the hot case. Also the recirculation zone shape changes also. This is

an effect of the volumetric expansion of the fluid element triggered by the chemical heat release through combustion [17], [18]. Also, the intensity of the swirl becomes smaller in the reactive case. As shown earlier, [5], combustion occurs rapidly at the vortex core, causing the density to drop via thermal expansion. Since the angular momentum is conserved, an increase in the vortex area results in a decrease of its intensity, effect that explains the differences in the vector field patterns in Fig. 5.

For a better understanding of this effect, a -5 m/s axial velocity isosurface is shown in Fig. 6. Significant changes in the shape of this region for the two simulated cases can be seen in Fig. 6, the recirculation zone reduces its radial dimension in the case with combustion (Fig. 6 b, c). As noted earlier, the heat release through chemical reaction increases the fluid volume in the region through thermal expansion, so one might have expected an increase in the recirculation region width. However, the heat release due to combustion accelerates the fluid flow in the stream around the recirculation region (Fig. 5 b). Furthermore, as the intensity of the swirl in the reactive case decreases, the increase in energy due to the addition of chemical energy it can be seen in the axial velocity mode. Simultaneously, the viscous effects are stronger in the reactive case due to the increase in temperature and therefore the transverse gradients of the axial velocity become larger and, thus, the higher axial velocity in the stream around the recirculation region entrains, axially, a larger part of the fluid from regions closer to the centerline, reducing the radial size of the recirculation region. Also one can see two structures that move radial (Fig. 6 b c). These structures are present in both cases, with and without combustion and appear on top of the largest cooling holes of the combustion chamber (Fig. 3, Fig. 6). This shows an unsteady behavior of the flow.

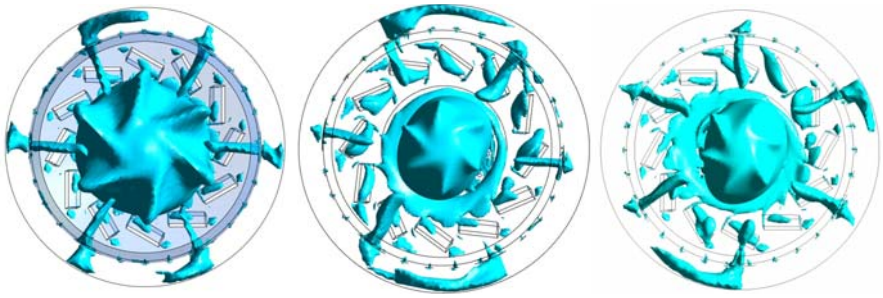

a b c

Fig 6. Iso-surface of the axial velocity at -5 m/s, (a) cold case, (b) hot case and (c) hot case

In order to address the recirculation region length issue, the axial velocity mean values were plotted against the appropriate spatial coordinate at different positions in the computational domain (Fig. 7). The horizontal line in Figure 7 is

placed at the combustor centerline, while the vertical lines are placed at 20, 60 and, respectively, 90 mm from the injector.

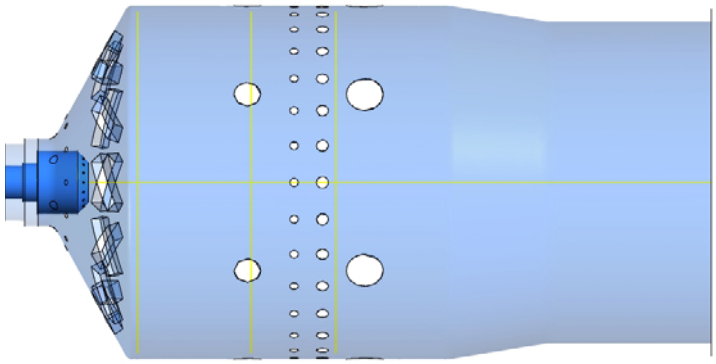

Fig. 7 Location of data plotted in Figures 7 - 10

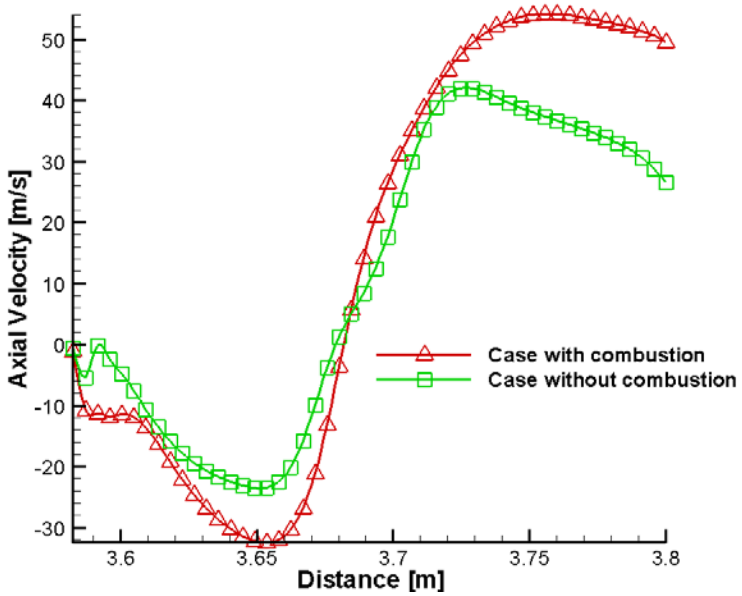

Fig. 8 Axial velocity profile on axial line

In Fig. 8 it is clearly seen that both the recirculation zone intensity and its length, are increasing in the combustion case. The axial velocity gradient is also higher in the reactive case, supporting the earlier presented considerations. Also the velocity at the exit is higher by about 20 m/s in the combustion case due to the additional energy release by chemical reaction.

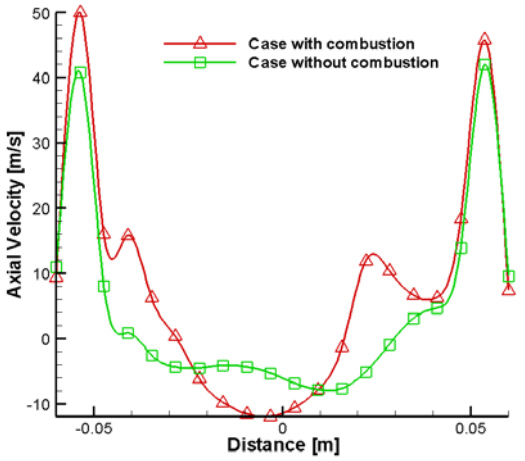

Fig. 9 Axial velocity profile at 20 mm from injector

In fig. 9, the recirculation zone is wider in the case without combustion but its intensity is higher in the other case. Also the fuel jet and the air jet are not completely merged into one jet in the case with combustion possibly because the velocity is higher in the region due to combustion. However the swirl angle is maintained in both cases.

The slight asymmetry of the solution is due to the highly turbulent flow in the domain and because of non-stationary phenomena. It is also important to note that the recirculation region is thicker in the non-reactive case (Fig. 7), and the transverse gradient of the axial velocity is higher for the reactive case, correlating with the earlier results and observations.

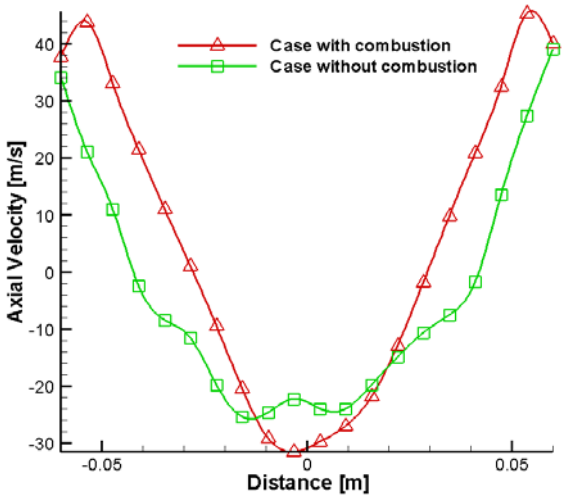

Fig.10 Axial velocity profile at 60 mm downstream from the injector

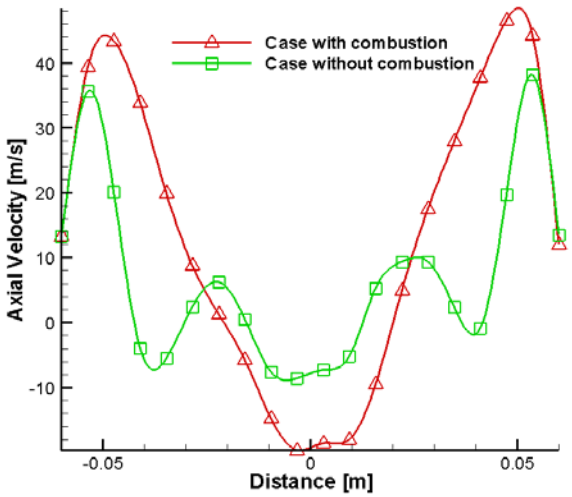

Fig. 11 Axial velocity profile at 90 mm downstream from injector

In Fig. 10, the velocity profile at this axial location shows that the recirculation zone is still wider in the case without combustion. The axial velocity transverse gradient remains larger in the combustion case, as expected.

In Fig. 11, it can be noted that the vortex breakdown is still strong in the combustion case while in the case without combustion is almost over if one corroborates it with Fig 4. Also the end of recirculation zone (Fig. 6 a) has an irregular termination, possibly influenced by the six cooling holes situated on circumference on the combustion chamber.

5. Conclusions

In this paper, numerically the flow inside an experimental combustion chamber, with and without combustion was analyzed. The results indicated a modification of the main recirculation zone in terms of shape and size. According to the results, the shape of it changes from truncated cone in the cold case to tear shape in the hot case (Fig. 4). And it can be observed a reduction of the recirculation zone thickness in the combustion case, with almost 15 % less than in the cold case. Also, the length of recirculation zone increase in the hot case by almost 10 % in the axial direction. The swirl number decreases, as expected, from 0.387 in the cold case to 0.108 in the hot case. Also, it can be noticed the presence of two structures (Fig. 6) that move radially on top of the largest cooling holes of the combustion chamber, showing an unsteady behavior of the flow, which means that an unsteady analysis is required further.

R E F E R E N C E S

[1] *M.G. Hall*, Vortex breakdown, Annual Review of Fluid Mechanics, **vol.** 4: 195-218, 1972

[2]*Ying Huang, Vigor Yang* - Dynamics and stability of lean-premixed swirl-stabilized combustion, Progress in Energy and Combustion Science, Volume 35, Issue 4, Pages 293–364, August 2009

[3] CFX Limited, Waterloo, Ontario, Canada, CFX-TASCflow Theory Documentation, Section 4.1.2, Version 2.12, 2002.

[4] *John C. Tannehill, Dale A. Anderson, Richard H. Pletcher*, Computational Fluid Mechanics and Heat Transfer, second edition, ISBN 1-56032-046-X (case)

[5] *P. A. McMurtry, W. H. Jou, J. J. Riley, and R. W. Metcalfe*, Direct numerical simulations of a reacting mixing layer with chemical heat release*,* AIAA Journal, **Vol**. 26 No. 6, pag. 962 - 970, 1985.

[6] *Ko, S.C. and Sung, H.J.,*Large-eddy simulation of turbulent flow inside a sudden-expansion cylindrical chamber, Journal of Turbulence, 3, 011, 2002

[7] *Szasz, R.Z., Duwig, C., and Fuchs, L.*, Numerical Simulation of reacting flows in Gas Turbine Burners with flame surface density model and LES, conference on Modelling Fluid flow (CMFF'03), Budapest, Hungary, September 3-6,2003

[8] *Gherman, B.G., Szasz, R.Z., Fuchs, L*., LES of Swirling flows in Gas Turbine combustion chambers, ASME Turbo Expo 2004, Vienna, Austria, June, 2004

[9] *R.K. Cheng.,* Ultraclean low-swirl combustion will help clear the air. Personal communication and EETD newsletter, 2003

[10] *G. Boudiera, L.Y.M. Gicquela, T. Poinsotb, D. Bissièresc, C. Bératc* Comparison of LES, RANS and experiments in an aeronautical gas turbine combustion chamber - Proceedings of the Combustion Institute Volume 31, Issue 2, Pages 3075–3082, January 2007

[11] *F. Wang, , L.X. Zhou, C.X. Xu* Large-eddy simulation of correlation moments in turbulent combustion and validation of the RANS-SOM combustion model – Fuel Volume 85, Issue 9, Pages 1242–1247, June 2006

[12] *Wei Wang, Tarek Echekki* Investigation of lifted jet flames stabilization mechanism using RANS simulations - Fire Safety Journal Volume 46, Issue 5, Pages 254–261, July 2011

[13] *V.L. Zimont, V. Battaglia* Joint RANS/LES approach to premixed flames modeling in the context of the TFC combustion model - Engineering Turbulence Modelling and Experiments 6 — Procedings of the ERCOFTAC International Symposium on Engineering Turbulence Modelling and Measurements - ETMM6 -Sardinia, Italy, 23–25 May, 2005

[14] *Khalid M. Saqra, Hossam S. Alyb, Hassan I. Kassema, Mohsin M. Siesa, Mazlan A. Wahida* Computations of shear driven vortex flow in a cylindrical cavity using a modified k-ε turbulence model - International Communications in Heat and Mass Transfer, Volume 37, Issue 8, Pages 1072–1077, October 2010

[15] *X. Bai & L. Fuchs* – Modeling of turbulent reactive flows past a bluff body: Assessment of accuracy and efficiency, Computers and Fluids, 23(3):507-521, 1994

[16] *Kato, M., Launder, B.E.* - The modelling of turbulent flow around stationary and vibrating square cylinders - Ninth Symposium on "Turbulent Shear Flows", Kyoto, Japan, August 16-18, 1993

[17] *F. C. Goldin, J.S. Depsky, S.L. Lee* , Velocity characteristics of a swirling flow combustor, AIAA journal, 23(1):95-102, 1985

[18] V. *Tangirala, R. Chen, J.F. Driscoll* , Effects of heat release and swirl on the recirculation within swirl-stabilized flames, Combust. Sci. and Tech., 51:75-95, 1987